NIH Public Access
Author Manuscript
J Phys Chem C Nanomater Interfaces. Author manuscript; available in PMC 2013 December 13.

Published in final edited form as:
J Phys Chem C Nanomater Interfaces. 2012 December 13; 116(49): 26102–26105. doi:10.1021/jp311269c.

Tunable Doping in Graphene by Light-Switchable Molecules

H. B. Mihiri Shashikala[†], **Chantel I. Nicolas**[‡], and **Xiao-Qian Wang**[*,†]

[†]Department of Physics, Clark Atlanta University, Atlanta, Georgia 30314, United States

[‡]Department of Chemistry, and Center for Functional Nanoscale Materials, Clark Atlanta University, Atlanta, Georgia 30314, United States

Abstract

Noncovalent functionalization provides an effective way to modulate the electronic properties of graphene. Recent experimental work has demonstrated that hybrids of dipolar phototransductive molecules tethered to graphene are reversibly tunable in doping. We have studied the electronic structure characteristics of chromophore/graphene hybrids using dispersion-corrected density functional theory. The Dirac point of noncovalently functionalized graphene shifts upward via *cis–trans* isomerism, which is attributed to a change in the chromophore's dipole moment. Our calculation results reveal that the experimentally observed reversible doping of graphene is attributed to the change in charge transfer between the light-switchable chromophore and graphene via isomerization. Furthermore, we show that by varying the electric field perpendicular to the supramolecular functionalized graphene, additional tailoring of graphene doping can be accomplished.

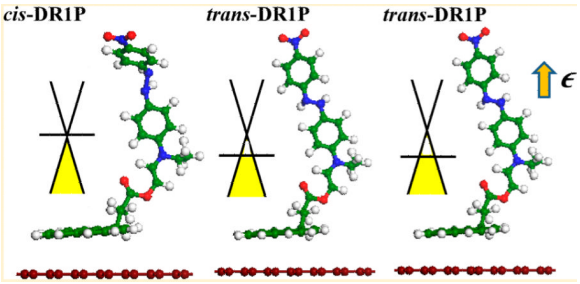

INTRODUCTION

Graphene is well-known for its unique properties, including its remarkable thermal conductivity, charge transport, and mechanical strength.[1-3] Graphene has a sp^2-hybridized planar network of carbons with extended π conjugation that makes it an ideal material for electronics applications.[1-6] Although covalent functionalization of graphene provides a way to tailor its electronic properties, the distortion of the sp^2 network remains difficult to control.[7-25] On the other hand, non-covalent functionalization of graphene is a controlled method whereby the π network is preserved, while the corresponding electronic properties are tuned by varying the dopant.[26-28] A controlled graphene doping technique is highly desirable for building stable devices with potential applications as biosensors and field-effect transistors.[29,30]

[*]**Corresponding Author**: xwang@cau.edu. .

The authors declare no competing financial interest.

Molecules with extended conjugated systems, such as pyrene, have been employed for noncovalent binding to graphene due to the π–π interactions between pyrene and gaphene sp^2-hybridized networks;[1,31] however, strong binding capability alone is not enough to achieve the desired effect due to pyrene's ineffectiveness as a dopant for practical applications.[32-34] One way to circumvent this issue is to utilize compounds derived from pyrene and dipolar molecules. The resulting pyrene derivative provides an opportunity to bind a strong dopant to graphene while preserving its unique electronic characteristics. Recent experimental work has shown that when tethered to the graphene's surface, the pyrene azo compound disperse red 1 pyrene (DR1P) is effective at modulating graphene doping via photoisomerization.[26] An increase in its dipole moment can be accomplished as the azobenzene-derived chromophore switches from a *cis* to a *trans* isomer, leading to distinctive doping behavior.[15,26] However, an in-depth understanding of these charge transfer interactions remains unclear.[33,34] Here, we report results based on dispersion-corrected density functional theory (DFT) calculations.[35] Our results shed further light on the correlation between changes in dipole moment and charge transfer. Moreover, we investigate the effect of applying a perpendicular electric bias to tune graphene's electronic properties.

COMPUTATIONAL DETAILS

We have performed calculations based on dispersion-corrected DFT to characterize structural and electronic properties. For the exchange-correlation functional, the gradient-corrected (GGA) Perdew–Burke–Ernzerhof (PBE) form was used.[35] To account for the interlayer van der Waals interactions, we utilized a dispersion correction that is based on the Tkatchenko–Scheffier (TS) scheme, which exploits the relationship between polarizability and volume.[36] The semi-empirial TS dispersion correction takes into account the relative variation in dispersion coefficients of various atomic bondings. It weights the values extracted from the high-quality ab initio database with atomic volumes derived from partitioning the self-consistent electron density.[36] The TS scheme has been successfully applied to a variety of systems for a much improved accuracy. Specifically, for graphite, local-density approximation overestimates the binding between the graphene layers, while GGA is very weak in binding.[37,38] Inclusion of the dispersion correction yields the correct layer distance of 3.719 Å, which is in good agreement with experiments.[37]

We have used a 7 × 7 rhombus cell that consistents of 98 carbon atoms and the DR1P molecule. The DR1P molecule has a pyrene group along with an azobenzene group. The DR1P has 35 carbon, 4 nitrogen, 32 hydrogen, and 4 oxygen atoms. Shown in Figure 1 are the optimized structures of *cis*-DR1P and *trans*-DR1P, respectively. As seen from Figure 1, the pyrene is nearly parallel to the graphene surface (with a slightly slanted angle of 6.5°). The azobenzene group serves as an optical switch to control the doping of the fractionalized graphene.[26] In the *cis*-DR1P conformation, the azobenzene group bends down, whereas the azobenzene group in the *trans*-DR1P stretches out. The stretched and bent conformations are characteristic of the light-switch molecule.[26] The dipole moment of 9D in the trans conformation of azobenzene reduced to 6D in *cis*.[26]

Furthermore, we have applied electric bias to both *cis*-DR1P and *trans*-DR1P. Using first-principles calculations, we found that in an applied electric field, the electrons of the *trans*-DR1P molecules are polarized. The quantum mechanical analysis for the description of a polarizable, neutral particle in a homogeneous electric field can be applied to an electrostatic potential distribution over the entire molecule.

Periodic-boundary conditions were employed with a super-cell in the *x*–*y* plane that was large enough to eliminate interactions between neighboring replicas. A double numerical

basis was sufficient for the grid integration of the charge density to converge. All structures were relaxed with forces less than 0.01 eV/Å.[33]

RESULTS AND DISCUSSION

The binding energy for *trans*-DR1P and *cis*-DR1P is −1190.6 and −1160.7 eV, respectively. The *trans*-DR1P has lower energy than *cis*-DR1P, and the isomerism can be induced by illumination of UV and white light.[26] The effect of doping can be readily clarified by the shift of the Dirac point in the band structure.[38] As seen from Figure 2, the Dirac point is located at the Fermi level in pristine graphene as well as in the *cis*-DR1P/graphene hybrid, whereas the corresponding Dirac point is shifted upward from the Fermi level in the *trans*-DR1P/graphene hybrid. The bands associated with the two DR1P isomers are characterized as flat bands, in contrast with the dispersed bands of graphene. For the *trans*-DR1P/graphene hybrid, there are two flat bands that are in close proximity to the Fermi level. Specifically, the two flat bands can be viewed as arising from the hybridization between graphene's π-band and the highest occupied molecular orbital (HOMO) and HOMO-1, respectively. The relative location of the HOMO-derived and HOMO-1-derived bands of DR1P plays an important role in electron doping. In this case, *trans*-DR1P provides a pool for electron doping because the HOMO-derived DR1P band is very close to the Fermi level. The strong doping of DR1P is also manifested in the amount of upward shift of the Dirac point. Furthermore, *trans*-DR1P has p-doping, whereas for *cis*-DR1P, there is no shift of the Dirac point, implying a much less effort of doping. As seen from the band structure (Figure 2), the HOMO-derived band of *trans*-DR1P is closer to the Fermi level, and the LUMO-derived band is located far above the Fermi level. The latter implies that the *trans*-DR1P serves as a charge donor to graphene.[37]

On the other hand, the two corresponding flat bands for the *cis*-DR1P/graphene hybrid are located relatively far away from the Fermi level and are separated from one another. Hence, the doping of graphene by the *cis*-DR1P is negligible. It is worth noting that there is no shift of the Dirac point for *cis*-DR1P-functionalized graphene. Although it is evident that the *cis*–*trans* isomerization yields changes in electronic doping, a quantitative characterization of the doping behavior through the shifts of Dirac point is useful.

To further pursue the charge transfer behavior, we illustrate in Figure 3 the isosurfaces associated with the valence band maximum (VBM) and conduction band minimum (CBM) of both *cis* and *trans*-DR1P/graphene. For the *trans*-DR1P/graphene hybrid, the VBM charge density is located on both the pyrene ring and the lower ring of the azobenzene group, whereas that of the *cis*-DR1P/graphene hybrid is concentrated on the whole azobenzene group only.

This difference in charge confinement is correlated with distinct doping behaviors. Charge transfer plays a major role in graphene doping by the *cis* and *trans* chromophores. To characterize charge transfer, we extract the Mulliken charges for both isomers, which are 0.01 and 0.02 *e* for the *cis*- and *trans*-DR1P/graphene hybrids, respectively (see Table 1). Charge transfer is more than twice as high for the *trans*-DR1P/graphene hybrid compared with the cis hybrid. It is worth noting that there exists intramolecular charge transfer between the pyrene and azobenzene rings, as well. The *trans* conformation of the azobenzene group allows for long-range charge transfer interactions between the two rings, thereby illustrating its distinct doping character. On the other hand, the corresponding charge transfer in *cis*-DR1P is much weaker due to its smaller dipole moment. These results are in agreement with experimental findings.[26] Specifically, it was found that the *trans*-DR1P isomer is a stronger hole dopant than *cis*-DR1P, which when tethered to the graphene's surface yields an ~18% decrease in doping without further synthesis.

Although DR1P/graphene hybrids are tunable through *cis–trans* photoisomerization, it is desirable to explore additional options to control graphene doping. To this end, we have investigated the effect of applying an electric bias. Shown in Figure 4 is the electronic structure of the *trans*-DR1P/graphene hybrid when an electric field of 0.05 and −0.05 V/Å is applied. The positive and negative electric biases correspond to the field directions from graphene to DR1P and from DR1P to graphene, respectively. Negative electric bias up-shifts the Dirac point of the structure by a factor of 2 higher than a positive electric bias, which indicates that this system can be further tuned with applied electric bias in addition to photoisomerism. Consequently, the dipole moment of *trans*-DR1P is altered by the electric field, thereby allowing the graphene sheet to donate electrons to *trans*-DR1P via the pyrene ring, which is a favorable direction for charge transfer.

The application of an electric bias in either direction enhances hole-doping as characterized by considerable shifts in the Dirac point. The *trans*-DR1P component undergoes intramolecular charge transfer as well as interlayer charge transfer. Specifically, with an electric field in the direction from graphene to *trans*-DR1P, the azobenzene ring becomes negatively charged, and the pyrene component shifts to being positively charged. In contrast, a negative electric bias has the opposite effect. Incremental increase in the electric bias leads to increased doping, as characterized by further Dirac point shifts, until a saturation point is eventually reached. This doping effect is more pronounced when a negative electric bias is applied. For *cis*-DR1P, the corresponding shift in the Dirac point with applied electric bias is not observed. This result contrasts with experimental findings, which report that there is an observed doping of graphene by *cis*-DR1P.[26] It is worth noting that the charge on the azobenzene component of *cis*-DR1P does not change with electric bias, indicating that its lower dipole moment renders it as an ineffective dopant.

CONCLUSION

In summary, DR1P/graphene hybrids are reversibly tunable with light and an applied electric field due to induced isomerism. Specifically, *trans*-DR1P was shown to have significant graphene doping capabilities. Electronic structures of both the *cis*- and *trans*-DR1P/graphene hybrids have been studied using dispersion-corrected density functional calculations. Our results show that *trans*-DR1P has a significant effect on hole doping, which is depicted by up-shifts of the Dirac point as compared with virtually no shift of the Dirac point when graphene interacts with *cis*-DR1P. Isosurface plots of the hybrids' CBM and VBM, together with Mulliken charge analysis, further confirm the distinct charge transfer hehavior.

Moreover, our results reveal that the electronic features of the *trans*-DR1P/graphene hybrid can be controlled with the use of an applied electric field, depending on its magnitude and direction. With an electric bias directed from *trans*-DR1P to graphene, charge transfer flows in a favorable direction and can be used in conjunction with phototransconduction to tune the properties of graphene. The additional control of the electronic properties of graphene doping as a function of electric bias should extend the range of distinctive physical phenomena and applications for nanodevices.

Acknowledgments

This work was supported by the National Science Foundation (Grant DMR-0934142), Air Force Office of Scientific Research (Grant FA9550-10-1-0254 to H.B.M.S. and X.Q.W.), and the NIH/NIGMS MBRS RISE (Grant R25-GM060414 to C.I.N.).

REFERENCES

(1). Geim AK. Science. 2009; 324:1530–1534. [PubMed: 19541989]

(2). Chen JH, Jang C, Xiao S, Ishigami M, Fuhrer MS. Nat. Nanotechnol. 2008; 3:206–209. [PubMed: 18654504]

(3). Hecht DS, Hu L, Irvin G. Adv. Mater. 2011; 23:1482–1513. [PubMed: 21322065]

(4). Bae S, Kim H, Lee Y, Xu X, Park J-S, Zheng Y, Balakrishnan J, Lei T, Kim HR, Song YI, Kim Y-J, Kim KS, Özyilmaz B, Ahn J-H, Hong BH, Iijima S. Nat. Nanotechnol. 2010; 5:574–578. [PubMed: 20562870]

(5). Kim M, Safron NS, Han E, Arnold MS, Gopalan P. Nano Lett. 2010; 10:1125–1131. [PubMed: 20192229]

(6). Bai J, Huang Y. Mater. Sci. Eng., R. 2010; 70:341–353.

(7). Simmons JM, In I, Campbell VE, Mark TJ, Léonard F, Gopalan P, Eriksson MA. Phys. Rev. Lett. 2007; 98:086802. [PubMed: 17359117]

(8). Liu H, Liu Y, Zhu DJ. Mater. Chem. 2011; 21:3335–3345.

(9). Guo B, Liu Q, Chen E, Zhu H, Fang L, Gong JR. Nano Lett. 2010; 10:4975–4980.

(10). Wei D, Liu Y, Wang Y, Zhang H, Huang L, Yu G. Nano Lett. 2009; 9:1752–1758. [PubMed: 19326921]

(11). Dong X, Fu D, Fang W, Shi Y, Chen P, Li L-J. Small. 2009; 5:1422–1426. [PubMed: 19296561]

(12). Meerholz K, Volodin BL, Sandalphon N, Kippelen B, Peyghambarian NV. Nature. 1994; 371:497–500.

(13). Lee M, Katz HE, Erben C, Gill DM, Gopalan P, Heber JD, McGee DJ. Science. 2002; 298:1401–1403. [PubMed: 12434054]

(14). Kolpak AM, Grossman JC. Nano Lett. 2011; 11:3156–3162. [PubMed: 21688811]

(15). Zhou X, Zifer T, Wong BM, Krafcik KL, Léonard F, Vance AL. Nano Lett. 2009; 9:1028–1033. [PubMed: 19206226]

(16). Guo X, Huang L, O'Brien S, Kim P, Nuckolls C. J. Am. Chem. Soc. 2005; 127:15045–15047. [PubMed: 16248641]

(17). Katsonis N, Kudernac T, Walko M, van der Molen SJ, van Wess BJ, Feringa BL. Adv. Mater. 2006; 18:1397–1400.

(18). Tsai C-S, Wang J-K, Skodje RT, Lin J-C. J. Am. Chem. Soc. 2005; 127:10788–10789. [PubMed: 16076158]

(19). Choi B-Y, Kahng S-J, Kim S, Kim H, Kim HW, Song YJ, Ihm J, Kuk Y. Phys. Rev. Lett. 2006; 96:156106. [PubMed: 16712175]

(20). Loudwig S, Bayley H. J. Am. Chem., Soc. 2006; 128:12404–12405. [PubMed: 16984176]

(21). Paoprasert P, Park B, Kim H, Colavita P, Hamers RJ, Evans PG, Gopalan P. Adv. Mater. 2008; 20:4180–4184.

(22). Zhang C, Du M-H, Cheng H-P, Zhang X-G, Roitberg AE, Krause JL. Phys. Rev. Lett. 2004; 92:158301–158304. [PubMed: 15169322]

(23). Fan Z-Q, Zhang Z-H, Qiu M, Deng X-Q, Tang G-P. Chin. Phys. Lett. 2012; 29:077305.

(24). Ryu S, Liu L, Berciaud S, Yu Y-J, Liu H, Kim P, Flynn GW, Bru LE. Nano Lett. 2010; 10:4944–4951.

(25). Panchakarla LS, Subrahmanyam KS, Saha SK, Govindaraj A, Krishnamurthy HR, Waghmare UV, Rao CN. Adv. Mater. 2009; 21:4726–4730.

(26). Myungwoong K, Safron NS, Huang C, Arnold S, Gopalan P. Nano Lett. 2012; 12:182–187. [PubMed: 22149166]

(27). Ferrari AC. Solid State Commun. 2007; 143:47–57.

(28). Das A, Pisana S, Chakraborty B, Piscanec S, Saha SK, Waghmare UV, Novoselov KS, Krishnamurthy HR, Geim AK, Ferrari AC, Sood AK. Nat. Nanotechnol. 2008; 3:210–15. [PubMed: 18654505]

(29). Adam S, Hwang EH, Galitski VM, Sarma SD. Proc. Natl., Acad. Sci. U.S.A. 2007; 104:18392. [PubMed: 18003926]

(30). Shi Y, Fang W, Zhang K, Zhang W, Li L-J. Small. 2009; 5:2005–2011. [PubMed: 19492352]
(31). Nduwimana A, Wang X-Q. ACS Nano. 2009; 3:1995–1999. [PubMed: 19548689]
(32). Morozov SV, Novoselov KS, Katsnelson MI, Schedin F, Elias DC, Jaszczak JA, Geim AK. Phys. Rev. Lett. 2008; 100:016602–016605. [PubMed: 18232798]
(33). Park S, Hu Y, Hwang JO, Lee ES, Casabianca LB, Cai W, Potts JR, Ha HW, Chen S, Junghoon O, Kim SO, Kim YH, Ishii Y, Ruoff RS. Nat. Commun. 2012; 3:638. [PubMed: 22273676]
(34). Hwang JO, Park JS, Choi DS, Kim JY, Lee SH, Lee KE, Kim YH, Song MH, Yoo S, Kim SO. ACS Nano. 2012; 6:159–167. [PubMed: 22148918]
(35). Perdew JP, Burke K, Ernzerhof M. Phys. Rev. Lett. 1996; 77:3865–3868. [PubMed: 10062328]
(36). Tkatchenko A, Scheffler M. Phys. Rev. Lett. 2009; 102:073005–073008. [PubMed: 19257665]
(37). Gunasinghe RN, Reuven DG, Suggs K, Wang X-Q. J. Phys. Chem. Lett. 2012; 3:3048–3052.
(38). Hargrove J, Shashikala HBM, Guerrido L, Ravi N, Wang X-Q. Nanoscale. 2012; 4:4443–4446. [PubMed: 22695708]

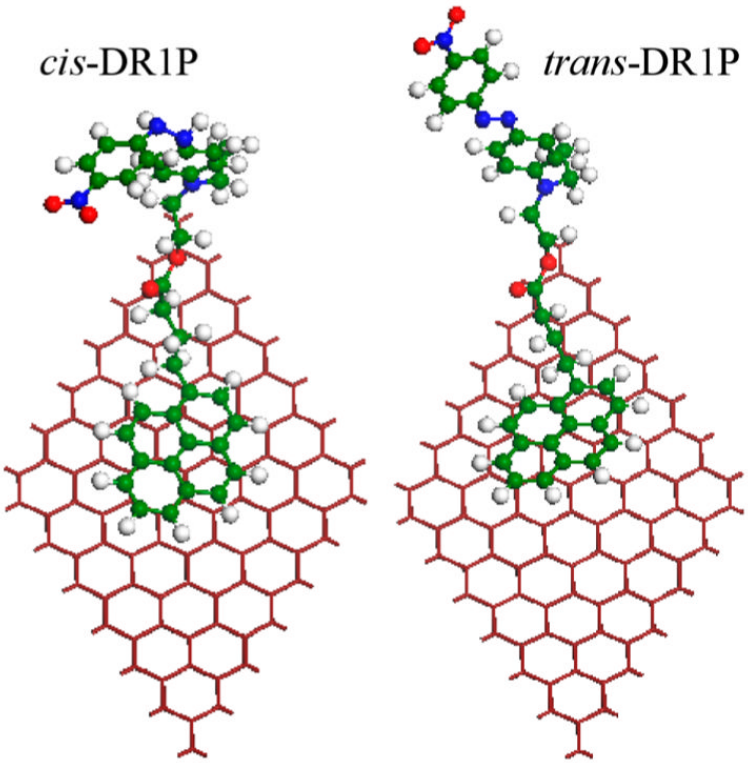

Figure 1.
Optimized structures of *cis*- and *trans*-DR1P isomers tethered to the graphene's surface in the left and right panels, respectively. Red, blue, and green spheres represent oxygen, nitrogen, and carbon atoms, respectively.

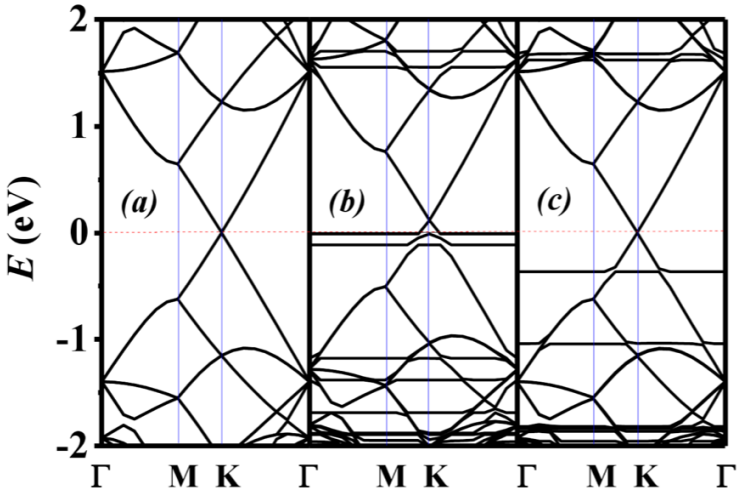

Figure 2.

Calculated band structures of (a) pristine graphene, (b) *trans*-DR1P on graphene, and (c) *cis*-DR1P on graphene, respectively. Γ = (0, 0), $K = (\pi/3a, 2\pi/3a)$, $M = (0, \pi/2a)$, where a = 17.220 Å. The Fermi level is shifted to 0 eV (red dashed line).

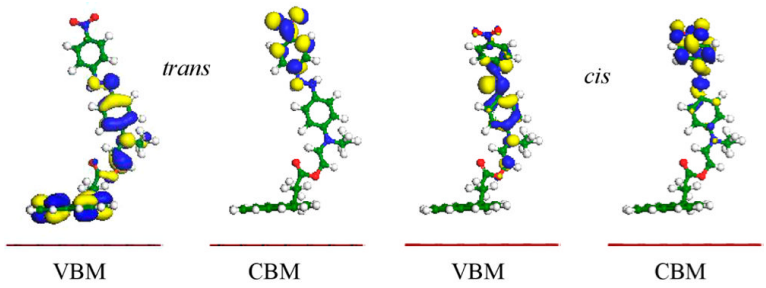

Figure 3.
Isosurfaces of the valence band maximum (VBM) and conduction band minimum (CBM) for *cis*- and *trans*-DR1P on graphene with 0.2 au isovalue.

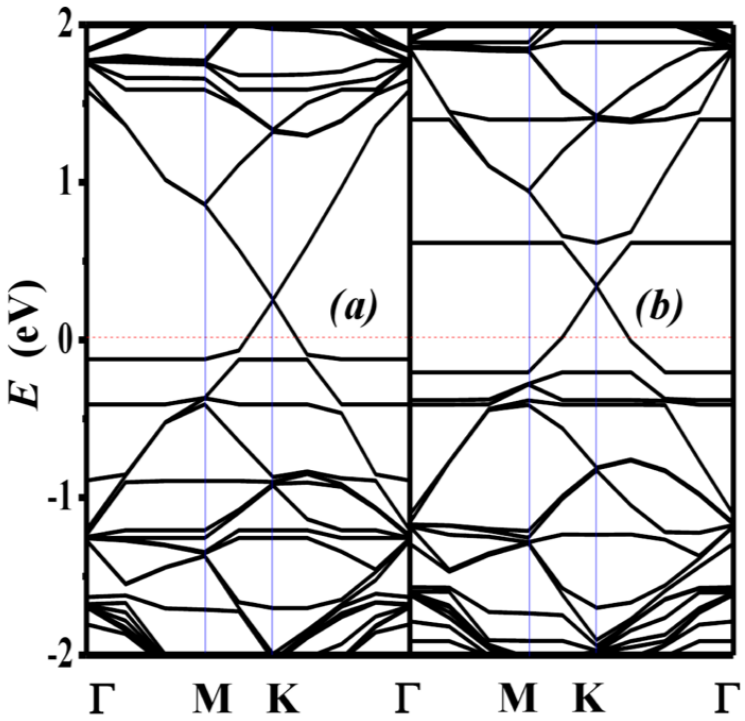

Figure 4.
Calculated band structure of *trans*-DR1P on graphene with electric biases of (a) 0.05 V/Å (from graphene to DR1P) and (b) −0.05 V/Å (from DR1P to graphene), respectively.

Table 1

Mulliken Charge of Individual Groups on *cis* and *trans*-DR1P/Graphene with Applied Electric Fields

	cis*-DR1P/graphene *(e)				***trans*-DR1P/graphene *(e)***			
electric field (V/Å)	**graphene**	**pyrene**	**azo-group**	***cis*-DR1P**	**graphene**	**pyrene**	**azo-group**	***cis*-DR1P**
0	0.000	0.238	−0.246	−0.008	−0.213	−0.38	0.247	0.209
0.05	0.001	0.222	−0.226	0.00	0.809	0.372	−1.180	−0.808
−0.05	−0.006	0.263	−0.226	0.001	0.780	−1.600	0.827	−0.773

J Phys Chem C Nanomater Interfaces. Author manuscript; available in PMC 2013 December 13.